Available online at www.sciencedirect.com
SCIENCE DIRECT®
Forest Ecology and Management 208 (2005) 189–209
Forest Ecology and Management
www.elsevier.com/locate/foreco

Estimating stand structure using discrete-return lidar: an example from low density, fire prone ponderosa pine forests

S.A. Hall[a,*], I.C. Burke[a], D.O. Box[b], M.R. Kaufmann[c], J.M. Stoker[d]

[a]*Graduate Degree Program in Ecology, Department of Forest, Rangeland and Watershed Stewardship, Colorado State University, Fort Collins, CO 80523-1472, USA*
[b]*Engineering and Technology Department, 3Di Technology Inc., Eagle Scan Remote Sensing, 1770 Range St., Suite B, Boulder, CO 80301, USA*
[c]*Rocky Mountain Research Station, USDA Forest Service, 240 W. Prospect Rd., Fort Collins, CO 80526, USA*
[d]*EROS Data Center, U.S. Geologic Survey, 47914 252nd St., Sioux Falls, SD 57198, USA*

Received 4 June 2004; received in revised form 2 December 2004; accepted 3 December 2004

Abstract

The ponderosa pine forests of the Colorado Front Range, USA, have historically been subjected to wildfires. Recent large burns have increased public interest in fire behavior and effects, and scientific interest in the carbon consequences of wildfires. Remote sensing techniques can provide spatially explicit estimates of stand structural characteristics. Some of these characteristics can be used as inputs to fire behavior models, increasing our understanding of the effect of fuels on fire behavior. Others provide estimates of carbon stocks, allowing us to quantify the carbon consequences of fire. Our objective was to use discrete-return lidar to estimate such variables, including stand height, total aboveground biomass, foliage biomass, basal area, tree density, canopy base height and canopy bulk density. We developed 39 metrics from the lidar data, and used them in limited combinations in regression models, which we fit to field estimates of the stand structural variables. We used an information–theoretic approach to select the best model for each variable, and to select the subset of lidar metrics with most predictive potential. Observed versus predicted values of stand structure variables were highly correlated, with r^2 ranging from 57% to 87%. The most parsimonious linear models for the biomass structure variables, based on a restricted dataset, explained between 35% and 58% of the observed variability. Our results provide us with useful estimates of stand height, total aboveground biomass, foliage biomass and basal area. There is promise for using this sensor to estimate tree density, canopy base height and canopy bulk density, though more research is needed to generate robust relationships. We selected 14 lidar metrics that showed the most potential as predictors of stand structure. We suggest that the focus of future lidar studies should broaden to include low density forests, particularly systems where the vertical structure of the canopy is important, such as fire prone forests.

Keywords: Carbon stocks; Fire-behavior-model input layers; Information–theoretic techniques; Lidar; Low density forests; Stand structure

* Corresponding author. Tel.: +1 970 491 7274; fax: +1 970 491 2156.
E-mail address: shall@cnr.colostate.edu (S.A. Hall).

0378-1127/$ – see front matter © 2004 Elsevier B.V. All rights reserved.
doi:10.1016/j.foreco.2004.12.001

1. Introduction

Most forests are subject to fire (Attiwill, 1994). The importance of fire, and its potential for releasing carbon stored in forest biomass, has become increasingly clear (Houghton et al., 2000). To quantify the role forests play in the global carbon cycle it is necessary to comprehend how fire affects carbon fluxes (e.g. net primary productivity and decomposition), and how these processes interact and feed back on each other. Studies of the effects of fire on the carbon cycle and on forest succession have been carried out in tropical (Hughes et al., 2000; Page et al., 2002), temperate (Keane et al., 1990) and boreal forests (Paré and Bergeron, 1995; Wirth et al., 1999), as well as in nonforested vegetation types (Tilman et al., 2000). Climate change is likely to interact with other factors and determine changes in fire regimes and post-fire productivity of many forests in the world (Overpeck et al., 1990; Flannigan and Van Wagner, 1991).

The ponderosa pine dominated forests at low elevations in the Rocky Mountains are historically fire prone (Covington and Moore, 1994). Over the last century, there have been significant changes in the structure of these forests (Weaver, 1959; Cooper, 1960; Kaufmann et al., 2000). Selective logging of large trees, grazing by domestic livestock, tree planting and fire suppression have all been identified as potential contributing factors that have led to an increase in stand densities and an accumulation of biomass and dead fuels in these forests (Covington and Moore, 1994). These changes have contributed to the recent occurrence of relatively large, severe wildfires in ponderosa pine forests. There are projects being developed and implemented to restore these forests to their historical condition, and reintroduce fire as a natural process (Moore et al., 1999; Fulé et al., 2001; Brown et al., 2001).

Quantification of the effect of fire on carbon stocks and fluxes requires estimates of the amount of biomass in ecosystem components, including actively photosynthesizing tissues. The development and use of spatially explicit maps of forest fuels can enhance our understanding and modeling of fire behavior (Perry, 1998). Given that fire is an inherently spatial process, restoration and fuel reduction efforts will be much more effective if the areas to be treated are selected based on data that include the landscape context of the area of interest. Therefore, there is a critical need to estimate structural variables of ponderosa pine forests. Total aboveground biomass, basal area and tree density provide information on carbon stocks. Foliage biomass, as an estimate of active tissues, is useful in estimating primary productivity. Stand height, canopy bulk density and canopy base height are common inputs for fire behavior models (Scott and Reinhardt, 2001). Stand height controls wind profiles within the forest; canopy base height is critical in determining whether the fire can reach the crowns of trees, and canopy bulk density quantifies the fuel in the canopy layer, which will feed active crown fires (Scott and Reinhardt, 2001).

Extensive, spatially explicit inventories of stand structure are extremely labor intensive and expensive. It is practically impossible to obtain full inventory coverage of large areas on the ground, especially where land ownership is mixed. One of the main advantages of remote sensing is the capacity to obtain spatially explicit data over large areas in a timely and economic fashion. These technologies have been used extensively in different forest types as a means to obtain spatially continuous estimates of stand structural variables (Franklin, 2001). Passive optical sensors (such as Landsat TM), as well as the techniques developed to estimate vegetation characteristics from the data they provide, have been around for many years (Wulder, 1998). Since these data are both inexpensive and reasonably available, most of the digital remote sensing research on estimating forest biophysical parameters has used these types of sensors. The capacity of these sensors is limited, however, because they provide two-dimensional information from which the three-dimensional structure of forests needs to be estimated. One consequence is that relationships developed to estimate total aboveground biomass or leaf area index are nonlinear, saturating at approximately 100 Mg/ha (Cohen and Spies, 1992) and 4 m^2/m^2 (Baret and Guyot, 1991; Spanner et al., 1994), respectively. A second consequence is that optical sensors cannot provide information on the vertical structure of biomass. This can be critical in determining fire behavior (van Wagner, 1977, 1993) and wildlife habitat potential (e.g. DeGraaf et al., 1998; Hershey et al., 1998).

Recent technological developments have led to a growing availability of active sensors, such as lidar (light detection and ranging) and radar. These sensors are designed to provide three-dimensional data, which makes them prime candidates for overcoming the saturation limitation of passive sensors (Dobson, 2000; Lefsky et al., 2001). Single wavelength radar has been used to estimate forest biomass, but has been shown to have similar limitations to those of passive sensors, saturating at approximately 150 Mg/ha (Waring et al., 1995).

Most topographic lidar sensors emit beams of infrared light, and measure the time it takes for the beamed energy to be reflected back to the sensor (Baltsavias, 1999a). The position and height of the reflecting surface is calculated based on the speed of light. There are two broad categories of lidar, large-footprint, continuous-return lidar, and small-footprint, discrete-return lidar (Lefsky et al., 2002b). The first class is characterized by the emission of a wide beam of light (tens of meters in diameter); the returning energy is stored as a height profile of intensity within that beam. These sensors include SLICER, LVIS, the proposed Vegetation Canopy Lidar and ICEsat (Lefsky et al., 2002b). Discrete-return lidar emits a small beam of light (centimeters in diameter), and records the positions from which the returned energy is greater than a certain threshold. Different systems can record from 1 to 5 discrete returns from each laser pulse. These systems are the ones commercially available (Baltsavias, 1999b), and are being used routinely to develop digital elevation models (Flood and Gutelius, 1997).

Both types of lidar have been used successfully to estimate stand structural variables, such as mean height, total aboveground biomass, basal area, stem volume and stand density, in a variety of forest types (Means et al., 1999, 2000; Lefsky et al., 1999a,b, 2002a; Dubayah and Drake, 2000; Drake et al., 2002, 2003; Naesset and Bjerknes, 2001; Naesset and Økland, 2002; Naesset, 2002). The focus of most of the research has been on overcoming the saturation at high biomass levels that limits the use of passive sensors, and no evidence of similar saturation has been found with lidar (Lefsky et al., 2002b). Little work has been done in forests of relatively low density, such as the ponderosa pine forests of the Front Range of Colorado, USA. Stoker (2002) developed models to accurately estimate individual tree height and diameter at breast height in these forests, using discrete, multiple-return lidar. This work needs to be extended to provide area-based estimates of total biomass, as well as other stand structural variables of interest for fire behavior modeling and carbon stock estimation. Our objective in this study was to estimate area-based structural variables using discrete, multiple-return lidar, and obtain a set of simple models to accurately estimate stand height, canopy base height, tree density, basal area, crown bulk density, total aboveground and foliage biomass in low density forests. Implicit in this objective is the selection of a subset of lidar-based metrics that were useful predictors of the structural variables of interest.

2. Methods

2.1. Study area

Our study area is in the Front Range of the Rocky Mountains, Colorado, USA. It is located east of the Cheesman Reservoir (39°11′N and 105°16′W), and comprises low elevation (2150–2400 m above sea level) montane forests, dominated by ponderosa pine (*Pinus ponderosa* Dougl. ex Laws), with a secondary component of Douglas-fir (*Pseudotsuga menziesii* (Mirb.) Franco). Mean annual rainfall is 413 mm, and mean monthly temperatures range from −2.9 to 18.5 °C (Western Regional Climate Center data, 1948–2004; http://www.wrcc.dri.edu/cgi-bin/cliMAIN.pl%3Fcochee).

2.2. Field data

We measured stand structure variables for 14 sites (mean area of 0.32 ha; Table 1) within the area of the overflight (see *Lidar data*, below) in the summer of 2001, distributed over a wide range of topographical positions (aspect and slope) and of structural conditions (Table 1). At each site we obtained measurements at 4–6 sampling points, randomly selected along a transect through the site, following the point-centered quarter method (Cottam and Curtis, 1956). Following this method, we estimated tree density from the point-to-tree distances (Cottam and Curtis, 1956). We recorded tree species, diameter at breast height,

Table 1
Range of topographical, stand and biomass structure conditions covered by the field data

Variables	Average	Minimum	Maximum
Slope (%)[a]	32	17	57
Aspect (° from N)[a]	157	37	311
Elevation (m, a.s.l.)[a]	2236	2157	2417
Area of site (ha)	0.32	0.16	0.75
Mean height (m)	12.6	8.1	17.2
Lorey's height (m)	15.7	12.7	21.2
Tree density (trees/ha)	329.7	90.0	1932.1
Basal area (m^2/ha)	19.4	9.8	73.1
Foliage biomass (Mg/ha)	7.4	3.3	31.1
Tree aboveground biomass (Mg/ha)	105.4	51.1	396.4
Canopy bulk density (kg/m^3)[a]	0.102	0.028	0.306
Canopy base height (m)[a]	3.3	0.45	11.25

[a] Only measured in the dataset collected in the summer of 2001 (14 sites). The rest of the variables were estimated for all 41 sites.

tree height, height to live crown and crown width for four trees (heights >3 m) selected at each point. Heights were measured with a Suunto® clinometer, while crown width and distances to trees (for density estimates and clinometer readings) were obtained with measuring tapes. We used allometric equations to estimate foliage and total tree aboveground biomass for each sampled tree (Table 2). From these individual tree values we obtained mean tree biomass, which we then multiplied by the estimated densities to obtain stand level (per hectare) values. From the measured values we calculated mean stand height (m), Lorey's height (basal-area-weighed average height, m; Husch et al., 2003), canopy bulk density (maximum 5-m running mean density of foliage, calculated for 0.3 m high intervals, kg/m^3; Scott and Reinhardt, 2001) canopy base height (minimum height with canopy bulk density greater than 0.037 kg/m^3, m; Sando and Wick, 1972), basal area (m^2/ha), total aboveground and foliage biomass (Mg/ha). At each site we also measured slope (with the Suunto® clinometer), aspect (compass bearing normal to the plane of the slope), latitude, longitude and elevation (with a Garmin GPS III+ handheld Global Positioning System, Garmin International Inc., Olathe, KS, USA). Latitude and longitude were used to match sites to the lidar data (see *Lidar data*, below).

We also used data collected in 1997 by Kaufmann and co-workers (unpublished), from a 15 ha stem-mapped plot within the study area. This dataset contains information on species, diameter at breast height and total height for each tree. The same allometric equations and calculations were applied to

Table 2
Allometric equations used to calculate foliage and total aboveground biomass for individual trees[a]

Biomass component	Allometric equations[b]	References
Pinus ponderosa		
Bole biomass (without bark)	$BB = BV \times \delta_w$	
	$BV = 3.25 \times 10^{-5}\ DBH^2\ H$	Edminster et al. (1980)
	$\delta_w = 537.58$ kg/m^3	this study
Bark biomass on bole	$\ln BkB = -4.2063 + 2.2312 \ln DBH$	Gholz et al. (1979)
Foliage biomass	$FB^c = (0.1167\ DBH^{1.5774}) \times 1.112$	Ter-Mikaelian and Korzukhin (1997)
Branch biomass	$BrB^c = (0.0469\ DBH^{2.1315}) \times 1.172$	Ter-Mikaelian and Korzukhin (1997)
Total aboveground biomass	$TAB = BB + BkB + FB + BrB$	
Pseudotsuga menziesii		
Bole biomass (without bark)	$\ln BB = -3.0396 + 2.5951 \ln DBH$	Gholz et al. (1979)
Bark biomass on bole	$\ln BkB = -4.3103 + 2.43 \ln DBH$	Gholz et al. (1979)
Foliage biomass	$FB^c = (0.3021\ DBH^{1.3076}) \times 1.158$	Ter-Mikaelian and Korzukhin (1997)
Branch biomass	$BrB^c = (0.2624\ DBH^{1.5464}) \times 1.244$	Ter-Mikaelian and Korzukhin (1997)
Total aboveground biomass	$TAB = BB + BkB + FB + BrB$	

[a] Mean tree values were multiplied by estimated tree density to provide stand level values.
[b] BB: bole biomass (kg); BkB: bark biomass (kg); FB: foliage biomass (kg); BrB: branch biomass (kg); TAB: total aboveground biomass (kg); DBH: diameter at breast height (cm); H: height (m); BV: bole volume (m^3); δ_w: wood density; ln: natural log.
[c] The constant by which the equation is multiplied is a bias correction factor published with these equations, as the models were fit as log transformed variables.

these data to obtain all structure variables except tree density, as in this dataset we had complete tree counts. From these data we obtained 27 stand level values for tree density, mean stand height, Lorey's height, basal area, and total and foliage biomass (each from 0.5 ha). Since this dataset did not contain values on height to live crown, we were unable to estimate canopy bulk density or canopy base height. We did not attempt to correct tree heights and diameters for growth occurred since measurements were taken, given the low growth rates of these forests. We assumed that the values of measurements in 2001 would not be greater than the 1997 values plus measurement errors.

2.3. Lidar data

The lidar sensor DATISII (3Di/EagleScan Inc.) was deployed over our sites on the 29th September 2001. It was configured to emit laser pulses (wavelength 1064 nm) with a frequency of 36.5 kHz. For each pulse, the system records information of up to five discrete positions where energy is returned to the sensor: easting and northing (datum WGS84; we used these to match these data with our field sites), height above sea level, return intensity and number of returns recorded for that pulse. The system is a scanning lidar, collecting data in only one direction across track. This configuration provided an average of 1.23 returns/m^2 (0.84–1.49 returns/m^2) for our sites. The swath width was approximately 1000 m (maximum angle was 15° from nadir). The horizontal position of each return has a root mean square error (RMSE) of 0.5 m (equal to the footprint diameter); the vertical RMSE is 0.15 m.

2.4. Processing of lidar data

Each return was automatically preclassified by 3Di/EagleScan as "ground" or "vegetation", and subclasses within each (proprietary algorithm). We generated contour lines with an interval of 0.01 m, based on a subset of the "ground" returns. We calculated the height above the ground for each return by subtracting the height of the nearest contour from the height above sea level. The small contour interval was selected to obtain ground height values directly below each return. Pairs of ground points that were within 40 cm horizontal distance of each other, and one of which was greater than 5 cm below the corresponding contour were considered representative of the same position, and their heights were averaged. If any of those points had originally been flagged as vegetation they were included in the "ground" set. The contours were then recalculated. This procedure was iterated until no "ground" return was more than 5 cm above or below its closest contour line. We used this stringent threshold to guarantee that interpolation errors did not surpass the vertical RMSE of the instrument.

For each site we calculated 39 metrics to synthesize the information contained in the cloud of discrete lidar points (Table 3; Appendix A). These metrics were developed based on the lidar literature (Lefsky et al., 1999a,b; Means et al., 1999, 2000; Naesset and Bjerknes, 2001; Naesset, 2002; Naesset and Økland, 2002; Drake et al., 2002) and modifications thereof. We decided to use as complete a set of metrics as possible, in an effort to set the stage for the convergence of studies using continuous- and discrete-return lidar. The development of lidar metrics for the different types of systems seems to have been relatively independent. Working under the assumption that the technology is likely to develop towards a small-footprint lidar with continuous profiling capacity, we attempted to provide a complete set of metrics that can be applied to all lidar systems, from which we intended to select those metrics most useful for predicting stand structure variables. We then grouped the 39 metrics based on their assumed relationship to different forest biophysical parameters (Table 3). The above processing was done in ArcView 3.2 (ESRI, Redlands, CA, USA).

2.5. Data analysis

We used an information–theoretic approach (Burnham and Anderson, 2002) to rank the regression models and select the best model to estimate each stand structural variable from lidar metrics. This methodology uses Akaike's Information Criterion (AIC) to rank a set of models developed a priori, based on the support provided by the field data. AIC is an estimate of the information lost when a model is used as an approximation to the truth, so the smaller the AIC value, the closer a particular model is to the (unknown) truth. The distance between models (in AIC units) provides information on whether the models ranked below the best one are close

Table 3
Composite metrics[a] derived from discrete cloud of lidar points to represent forest biophysical parameters

Biophysical parameter represented	LiDAR-based metrics
Height	
Mean tree height	h_{25}: mean height of all 1st "vegetation" returns from multiple-return pulses, with height >3 m[b] h_{35}: mean height of all 1st "vegetation" returns from pulses with 3 or more returns, with height >3 m[b]
Mean canopy height	h_1: mean height of all 1st returns classified as vegetation h_3: mean height of all 1st returns with height >3 m[b] h_{12}: mean height of all 1st "vegetation" returns from 2-return pulses h_{13}: mean height of all 1st "vegetation" returns from 3-return pulses h_{1m}: mean height of all 1st "vegetation" returns from multiple-return pulses QMCH: quadratic mean canopy height: mean standardized intensities[c] per height bin (0.5 m), weighed by the square of the height of the bin[d] CH: mean height of the highest "vegetation" return in each m^2
Maximum tree height	h_{max}: height of the highest return in the site
Cumulative canopy height	h_{maxi}: mean height of the highest i% of 1st "vegetation" returns (i = 5, 10, 25, 50, 75, 90, 95)
Median canopy height	medCH: height of the midpoint of the 0.5 m tall height bin with 50% of cumulative standardized intensity of returns (defined in Appendix A) above it and 50% below it
Crown height	HC: height of the midpoint of the 0.5 m tall bin with the minimum number of "vegetation" returns
Variability in canopy height	SD_{h_3}[e]: standard deviation in height of returns used to calculate h_3 CV_{h_3}: SD_{h_3}/h_3 $range_{h_3}$[e]: range of heights of returns used to calculate h_3 rel-$range_{h_3}$: rel-$range_h/h_3$
Biomass density	CRS: canopy reflection sum: sum of intensity of all returns reflected by the canopy[d] CRS_3: canopy reflection sum, considering only returns higher that 3 m[b] rel-CRS_1: canopy reflection sum relative to total reflection intensity (i.e. reflected by both the canopy and the ground)[d] rel-CRS_2: rel-CRS_1, corrected for ground surface reflectance (sensu Lefsky et al., 1999b)[d] wCRS: weighted canopy reflection sum: similar to CRS, but the intensity of each return is weighed by the inverse of its height above the ground[d] RperP: number of "vegetation" returns, relative to the number of pulses δ_{veg}: number of "vegetation" returns per unit area δ_{12}, δ_{13}, δ_{1m}: number of 1st "vegetation" returns from pulses with 2, 3, or multiple returns, respectively, per unit area δ_3: number of returns with height >3 m[b] per unit area (initially considered metric for tree density)
Canopy cover	CR_1: proportion of total energy returned reflected by the canopy[d] CR_2: CR_1, corrected for ground surface reflectance (assumed to be half the reflectance of the canopy; sensu Lefsky et al., 1999b)[d] δ_{11}: density of returns from 1-return pulses $P_{G/1}$: proportion of ground returns that are also 1st returns $P_{1/G}$: proportion of 1st returns that are also ground returns

[a] These metrics were used in models to predict stand structural variables.
[b] Height threshold follows sampling decisions in the field: only trees greater than 3 m in height were sampled.
[c] Standardized intensities: intensity of a single return, expressed as the proportion of the total intensity returned for that particular pulse.
[d] Rationale and calculations developed in Appendix A.
[e] Absolute measures of variability.

competitors or not. A rough guide is that models within 1–2 AIC units of the best model have substantial support; models 3–7 units from the best model have less support, and models more than 10 units away from the best model have essentially no support (Burnham and Anderson, 2002). In this way, this methodology provides more useful information than other commonly used techniques, such as stepwise regression. We focused our interpretation of results on models within three AIC units of the best model, as having equivalent support in the data.

This is an exploratory analysis, and the incorporation of a large number of predictor variables (39 lidar metrics) might lead us to find spurious relationships. Our use of the information–theoretic approach is geared precisely at trying to avoid these spurious relationships. Even for the structural variable for which we developed the largest number of models, this number is lower than the combinations of variables that would be considered if we ran stepwise regression procedures using only six independent variables. The critical advantage of our chosen methodology is that we had control, a priori, of the combination of metrics we used within a single model, as well as the number of predictor variables within each model. Though this is not a guarantee against these models portraying spurious relationships, they are at least based on a mechanistic hypothesis of why they should be good predictors of each stand structural variable. Therefore, the only uncertainty left is whether the resulting correlations are due to the hypothesized causations.

This methodology also provides information on model selection uncertainty, using the Akaike weights (w_r). These quantify the uncertainty related to whether the selected best model is the actual best model. They can be interpreted as the probability that the best model would again be selected as the best model, given the same set of candidate models and another sample of similar data (Burnham and Anderson, 2002).

For each stand structural variable, we fitted a variety of statistical models to the field data, using lidar metrics as independent variables and each stand structural variable of interest as the dependent variable. These models included linear models with up to three independent variables, and power functions of single metrics. The variables and combinations used for each stand structural variable are described in Appendix B. We log-transformed the stand structure variables to obtain homogeneity of variance and normality of residuals where necessary. Where variables were log-transformed, the fitted model was modified accordingly, to obtain the proposed relationship between dependent and independent variables (e.g. if the proposed model was $y = b_0 + b_1x$, then the model we fit was $z = \log(b_0 + b_1x)$, where $z = \log(y)$ and log is the natural log. In Section 3, the model would be expressed as $y = b_0 + b_1x$. We estimated the bias introduced by the transformation (Sprugel, 1983), and used these estimates to correct the predictions.

AIC is calculated based on estimates for model parameters obtained by fitting the data using maximum likelihood techniques. Given the structure of the field data (all variables were either normally or log-normally distributed), we used least squares techniques to fit the models, and estimated the likelihood of each model given the field data as:

$$\log(\ell(\hat{\theta})) = -\frac{n}{2}\log(\hat{\sigma}^2)$$

where $\ell(\hat{\theta})$ is the likelihood of the model given the data, n the sample size and $\hat{\sigma}^2$ is the residual sum of squares divided by the sample size. Note that the maximum likelihood estimates of the parameters do not change under log transformations, as the density functions differ only by a multiplicative constant that does not depend on the parameter (Lindgren, 1993; Section 12.1). This constant additively modifies the absolute value of the $\log(\ell(\hat{\theta}))$. We fitted the regression models using the procedure for nonlinear estimation in SAS (NLIN; SAS Institute Inc., Cary, NC, USA). We calculated the AIC for each model, and corrected these values for bias due to small sample sizes (AIC_c):

$$AIC_c = -2\log(\ell(\hat{\theta})) + 2K + \frac{2K(K+1)}{(n-K-1)}$$

where K is the number of estimated parameters (including an estimate of variance). We ranked the models based on AIC_c, and calculated the Akaike weights for each model as:

$$w_r = \frac{e^{-0.5(AIC_r - AIC_{min})}}{\sum_{i=1}^{R} e^{-0.5(AIC_i - AIC_{min})}}$$

where AIC_r is the model's AIC_c, AIC_{min} the minimum AIC_c of all the models in the candidate set, and R is the number of candidate models. The additive constant in

the $\log(\ell(\hat{\theta}))$ for the log-transformed variables affects the absolute value of AIC_c, but not the ranking of the models.

3. Results

3.1. Stand height

The best regression model for mean stand height explained slightly under 60% of the variability of the 41 sites (Table 4; Fig. 1a), based on two independent variables: the mean height of the upper 50% of 1st "vegetation" returns (h_{max50}) and the standard deviation of all 1st returns with height >3 m (SD_{h_3}). This model had only a 9% chance of being the best model, and eleven other models had equivalent support (Table 4). The first four competing models had the same structure as the best model, with a different cumulative height or variability metric (Table 4). The rest of the top models with significant coefficients (i.e. the 95% confidence limits did not straddle zero) were functions of a single cumulative height metric.

Expressing stand height as the basal-area-weighed average tree height (Lorey's height) increased the fit of the best model (r^2 = 86.8%), and slightly improved the probability that the model was the best one from the candidate set (w_r = 0.16) (Table 4; Fig. 1b). The best model for Lorey's height was a linear function of the mean height of the highest 25% of the 1st "vegetation" returns (h_{max25}; Table 4). Another eight models had similar support in the data (Table 4). They all had h_{max25} as a predictor. The last six of these had an added predictor, representative of variability in canopy height (Table 4). They are equivalent to the best model, though, since the confidence limits of their added coefficients straddled zero.

3.2. Biomass structure variables for estimates of carbon stocks

We analyzed four descriptors of stand biomass structure commonly used to quantify carbon stocks and fluxes: total aboveground biomass, basal area, tree density and foliage biomass. All were log-transformed previous to the analysis. The best model for each biomass structure variable explained between 67.2% and 79.4% of the variability of the 41 sites (Table 4; Fig. 2). The best model for these four structural variables was a negative exponential function of the proportion of ground returns that were not intercepted by the canopy ($P_{G/1}$). The model selection uncertainty

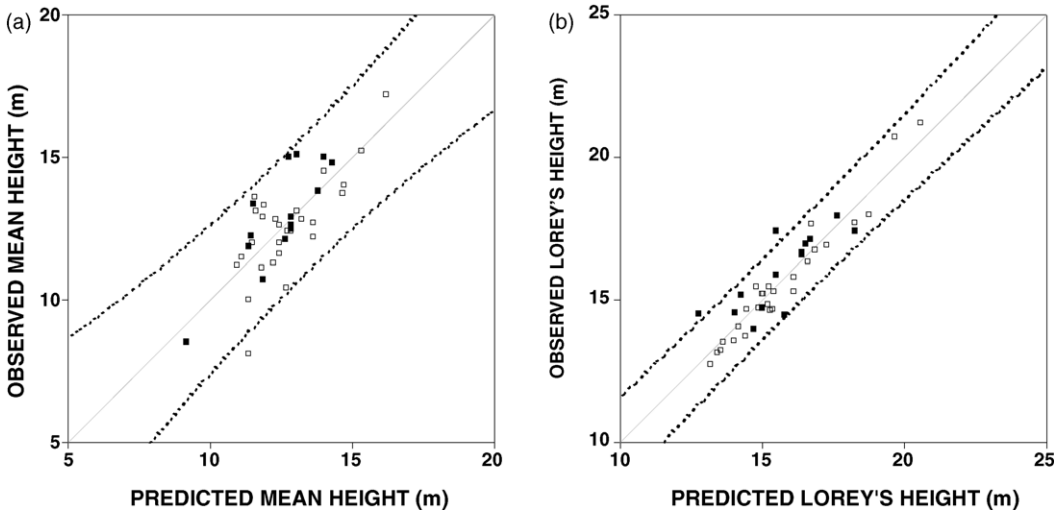

Fig. 1. Observed values of stand height vs. values predicted by the best regression model. (a) Mean height of sampled trees. (b) Basal-area-weighed average height (Lorey's height) of sampled trees. Full and empty squares represent the two sets of data used (14 and 27 points, respectively). The solid gray line represents the 1:1 line, where observed = predicted. The dotted black lines are the limits of the 95% prediction intervals for the plotted model. Models are presented in Table 4.

Table 4
Top models describing each stand structure variable

Stand structure (dependent) variable	Best regression model[a]	Coefficients (standard error)				w_r[b]	r^2[c]	S.E.[d]	Number of competing models[e]	Predictor variables in competing models[f]
		b_0	b_1	b_2	c					
Mean stand height (m)	$b_0 + b_1 h_{max50} + b_2 SD_{h_3}$ (5)	4.52 (1.40)	0.82 (0.12)	−0.78 (0.36)		0.09	57.1	1.18	11	h_{max75} (2), $_{95,90,25,10}$, CV_{h_3}, $range_{h_3}$ (1)
Lorey's height (m)	$b_0 + b_1 h_{max25}$ (9)	1.90 (0.87)	0.86 (0.05)			0.16	86.8	0.69	8	SD_{h_3}, $range_{h_3}$ (2), CV_{h_3}, rel-$range_{h_3}$ (1)
Total aboveground biomass (Mg/ha)	$b_1 P_{G/1}$[c] (2)		35.79 (3.61)		−2.67 (0.25)	0.56	74.2	0.20	1	–
Foliage biomass (Mg/ha)	$b_1 P_{G/1}$[c]		2.06 (0.20)		−3.06 (0.25)	>0.99	79.4	0.20	0	–
Basal area (m^2/ha)	$b_1 P_{G/1}$[c]		6.17 (0.57)		−2.76 (0.23)	>0.99	78.5	0.19	0	–
Tree density (trees/ha)	$b_1 P_{G/1}$[c]		56.39 (9.94)		−3.94 (0.44)	>0.99	67.2	0.36	0	–
Canopy base height (m)	$b_0 + b_1 h_{1m} + b_2 SD_{h_3}$ (1)	0.27 (1.83)	−0.57 (0.08)	2.20 (0.51)		0.39	79.8	0.36	1	h_{13}, $range_{h_3}$ (1)
Canopy bulk density (kg/m^3)	$b_1 P_{G/1}$[c]		0.018 (0.004)		−3.45 (0.45)	0.56	82.8	0.32	0	–

[a] Independent variables follow names in Table 3. In parentheses is the number of competing models these variables formed part of.
[b] Akaike weights (probability that the model would be selected as the best model from the same candidate set, given another dataset).
[c] Coefficient of determination of the regression. Values are in natural log space for all variables except mean stand height and Lorey's height.
[d] Standard error of estimates. Values are in natural log space for all variables except mean stand height and Lorey's height (m).
[e] Competing models are defined as those within 3 AIC_c units of the best model (number does not include the best model).
[f] Variables are ordered by the number of competing models they form part of, which is shown in parentheses.

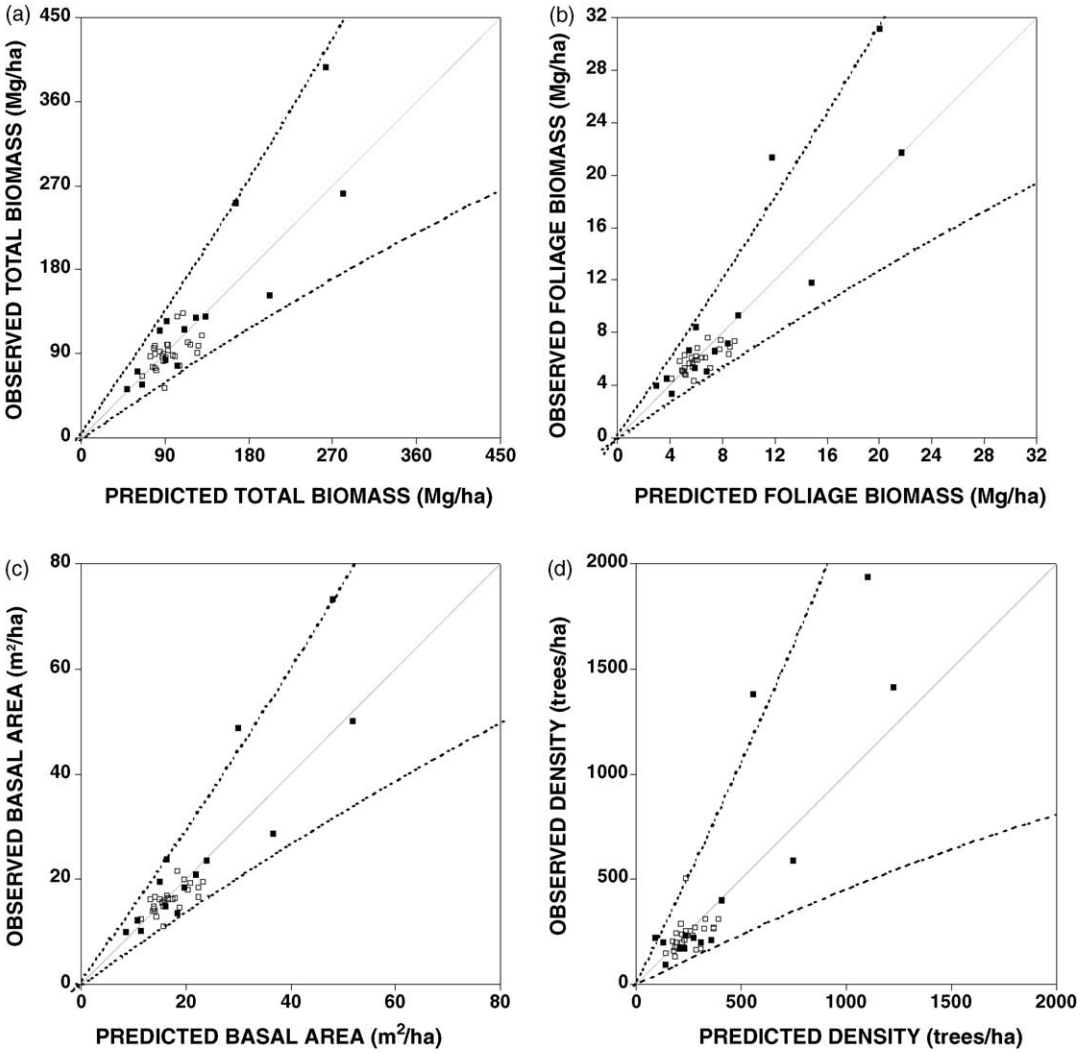

Fig. 2. Observed values of biomass structure variables vs. values predicted by the best regression model. The biomass structure variables analyzed were: (a) total tree aboveground biomass (Mg/ha); (b) foliage biomass (Mg/ha); (c) basal area (m^2/ha); (d) tree density (trees/ha). Full and empty squares represent the two sets of data used (14 and 27 points, respectively). The solid gray line represents the 1:1 line, where observed = predicted. The dotted black lines are the limits of the 95% prediction intervals for the plotted model. Model coefficients are presented in Table 4.

for tree density, basal area and foliage biomass was negligible ($w_r > 0.99$). The uncertainty was greater for total aboveground biomass ($w_r = 0.56$). The regressions of predicted versus observed values of all four variables did not follow the 1:1 line consistently (Fig. 2). There were four sites with substantially greater biomass and density than the other 37 (Fig. 2). These were four out of five leverage points identified using objective diagnostics (ROBUSTREG procedure, SAS, SAS Institute Inc., Cary, NC, USA). To analyze the effect of these values on the regression coefficients and, particularly, on the selection of models, we refit and reranked the models without these five leverage points (i.e. based on what we will call the restricted dataset). For all four biomass structure variables, the new regression coefficients of the original best model were outside the approximately 95% confidence limits of the original values. The coefficient of determination of the best models decreased in all cases (Table 5).

Table 5
Goodness of fit of original best models when fitted to the restricted datasets[a]

Dependent variable	N	r^2 [b]	S.E.[c]
Total aboveground biomass (Mg/ha)	36	37.9	0.18
Foliage biomass (Mg/ha)	36	53.8	0.14
Basal area (m^2/ha)	36	48.1	0.14
Tree density (trees/ha)	36	33.8	0.26

[a] We restricted the data by eliminating five leverage points (the same five for all response variables) to determine their effect on model parameters and ranking.
[b] Coefficient of determination of the regression (in natural log space).
[c] Standard error of estimates (in natural log space).

The models selected for total aboveground biomass and basal area with the restricted dataset were almost all linear. The top seven models for total aboveground biomass were functions of a height metric and a metric related to canopy cover, and all explained approximately 60% of the variability. The top 15 models for basal area had r^2 ranging from 48.1% to 57.8%. The equivalent to the original best model for basal area was ranked tenth. A linear function of the same independent variable was ranked 7th. The rest of the top models linearly combined a height metric with a canopy cover or biomass density metric (some with interaction terms), similar to the models for total aboveground biomass (Table 6).

The best model for tree density was again a nonlinear function of a canopy cover related metric. The linear function of the same variable was a close competing model, though the fit of both models was low (Table 6). A linear function of a height metric, a cover metric and a crown height metric was the best model for foliage biomass. The linear version of the original best model for foliage biomass was within one AIC_c unit of the best model.

3.3. Fire behavior modeling variables

The values for the two main fire behavior model inputs, canopy base height and canopy bulk density, were log-transformed. One of the 14 sites for which we had measurements of height to live crown (required to estimate both canopy base height and canopy bulk density) did not have densities greater than 0.037 kg/m^3 at any height (threshold value used to define canopy base height; Sando and Wick, 1972), so we were unable to calculate its canopy base height. Therefore, the regressions for this variable were fitted to 13 points.

The best model describing canopy base height was linear, with two independent variables: the mean height of 1st "vegetation" returns from multiple-return pulses (h_{1m}) and the standard deviation of the heights of all 1st returns more than 3 m from the ground (SD_{h_3}; Table 4). This model had a 39% chance of being selected as the best model using another dataset. Only one other model had equivalent support in the data (Table 4): a function of the mean height of 1st "vegetation" returns from 3-return pulses (h_{13}) and the range in height of all 1st returns more than 3 m from the ground ($range_{h_3}$), with an interaction term.

The coefficient of determination of the best model for canopy base height seemed to be dominated by two sites, with canopy base height (CBH) values of 11.25 m and 0.45 m (Fig. 3). We were unable to objectively determine if these were leverage points, as we did for the C stock variables above, since the log-transformation of this linear model is nonlinear, and

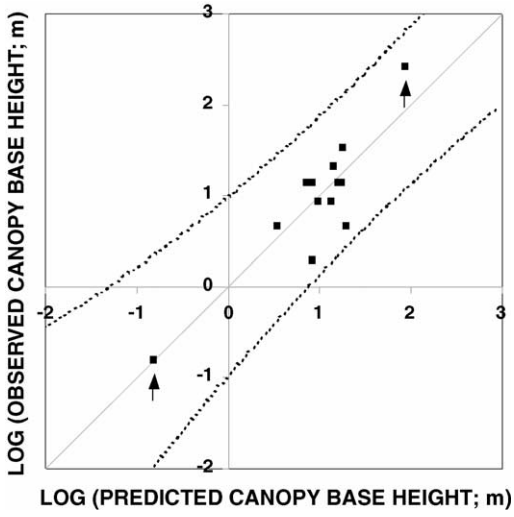

Fig. 3. Observed values of canopy base height (CBH) vs. values predicted by the best regression model, in natural log space. The arrows identify the two points we suspected might have undue influence on the regression fit and model ranking. The solid gray line represents the 1:1 line, where log (observed) = log (predicted). The dotted black lines are the limits of the 95% prediction intervals for the original best model ($N = 13$). The model is presented in Table 4.

Table 6
Most parsimonious model describing each stand structure variable, fitted to the restricted datasets[a] [$N = 36$ for all variables except canopy base height ($N = 12$)]

Stand structure (dependent) variable	Best regression model[b]	Coefficients (standard error)			w_r[c]	r^2[d]	S.E.[e]	Distance from best model[f]	Number of competing models[g]	Predictor variables in competing models[h]
		b_0	b_1	b_2						
Total aboveground biomass (Mg/ha)	$b_0 + b_1\mathrm{CH} + b_2P_{1/G}$ (2) (4)	90.62 (14.96)	9.33 (1.63)	−185.0 (31.06)	0.11	58.1	0.14	0	6	CR_2 (3), $h_{max95,90}$ (2), h_1 (1)
Foliage biomass (Mg/ha)	$b_0 + b_1P_{G/1}$ (4)	17.63 (1.83)	−16.64 (2.53)		0.04	54.5	0.14	0.6	3	HC (2), h_{max}, h_{25} (1)
Basal area (m^2/ha)	$b_0 + b_1\mathrm{CH} + b_2P_{1/G}$ (2) (6)	19.43 (2.51)	1.12 (0.27)	−30.3 (5.27)	0.03	49.8	0.14	1.3	14	medCH, h_{max90} (4), RperP (3), rel-CRS_2, h_{max95}, $P_{G/1}$ (2), h_1, rel-CRS_1 (1)
Tree density (trees/ha)	$b_0 + b_1P_{1/G}$ (2)	418.5 (50.41)	−482.7 (110.1)		0.25	34.9	0.26	1.1	3	$P_{G/1}$ (2)
Canopy base height (m)	$b_0 + b_1h_{1m} + b_2\mathrm{SD}_{h_3}$ (2)	1.75 (2.06)	−0.54 (0.07)	1.70 (0.56)	0.37	76.2	0.33	0	3	h_{13} (1)

[a] We restricted the data to determine their effect on model parameters and ranking. We eliminated five leverage points for all four C stock variables (the same five for all response variables). For canopy base height, we eliminated one high value, subjectively considered a potential outlier.
[b] Independent variables follow names in Table 3. In parentheses is the number of competing models these variables formed part of.
[c] Akaike weights (probability that the model would be selected as the best model from the same candidate set, given another dataset).
[d] Coefficient of determination of the regression (in natural log space).
[e] Standard error of estimates (in natural log space).
[f] Distance, in AIC_c units, that the most parsimonious model is from the model ranked as best.
[g] Competing models are defined as those within 3 AIC_c units of the best model (number does not include the selected model).
[h] Variables are ordered by the number of competing models they form part of, which is shown in parentheses.

the software used does not provide diagnostics for nonlinear models. The reanalysis described below must therefore be considered tentative. The results of refitting and reranking the models without the high value supported the same best model (Table 6), and the regression coefficients were within one standard error of the original values. The models that resulted from rerunning the analysis without both the large and the small value had very low goodness of fit; the best model explained 12.4% of the variability. The range of predicted values was substantially smaller than that of the observed (1.1 m versus 3.3 m).

We had estimates of canopy bulk density for all 14 sites measured in the summer of 2001. The best model was a negative exponential function of the proportion of ground returns that were not intercepted by the canopy ($P_{G/1}$; Table 4), which was the same as the best models for the biomass structure variables. This model explained 82.8% of the variability (Table 4), and there were no identifiable leverage points in the data. The Akaike weight for the best model was 0.56. The linear function of this same predictor variable ($P_{G/1}$) was not a close competitor, though it was within 10 AIC_c units of best model. A linear function of a biomass density variable (δ_{12}; Table 3) was within 6 AIC_c units of the best model.

4. Discussion

4.1. Predictors for C stock and fire behavior modeling variables

The cumulative height metrics in the top models for mean tree height were the lower fractions of returns ($\leq$50%), and are therefore, dominated by reflection from the upper canopy (i.e. the height of large trees). Stands with greater variability in canopy surface height are likely composed of large trees, mixed in with gaps filled by smaller trees. The mean height of these stands is likely lower than the cumulative height metric would suggest, as the height of those smaller trees needs to be incorporated. This explains the selection of a model where mean height is positively related to a cumulative height metric and negatively related to variability in height.

The discrete lidar points provide information on the integrated stand, and are therefore, dominated by the large trees that form the surface of the canopy. The values of Lorey's height are dominated by the height of large trees, and therefore, are more consistent with the height information provided by the lidar data than the mean height values. The goodness of fit of our models for Lorey's height was similar to those found by Stoker (2002) for lidar-identified individual tree heights (these probably represent clumps of trees indistinguishable from each other with lidar data). Lidar-derived heights explained 91% of the variability in height of known individual trees (Stoker, 2002).

We used the mean height of cumulative fractions of 1st returns (h_{maxi}; Table 3) as predictor variables in an effort to select those returns that characterize the surface of the canopy. Our results for Lorey's height indicate that the tallest 25% of 1st returns (h_{max25}) are a good approximation to this surface. We suggest that these cumulative height metrics should be more robust than percentile heights, such as those used in other studies (Naesset, 2002; Naesset and Økland, 2002). The fraction of returns that represent the canopy surface should be a function of only canopy cover of the dominant trees, while the percentile heights are a function of the complete, three dimensional leaf area index profile (Magnussen and Boudewyn, 1998).

Nonlinear functions of h_{max25} and models with two predictor variables were close competitors to the best model for Lorey's height. However, there are reasons to support the use of the simple, linear model, even given its model selection uncertainty. First, the high model selection uncertainty is likely due to the large number of candidate models we included in this analysis. Second, lidar measures height directly (Lefsky et al., 2002b), and other studies have found strong linear relationships ($r^2 > 90\%$) between lidar height metrics and stand height (Means et al., 1999, 2000; Holmgren et al., 2003).

Our capacity to predict canopy base height from lidar metrics was limited. The fit of the original best model was very good, but this seemed to be dominated by two sites with extreme values. Given the consistency of results with and without the large value, and the lack of fit without both extremes, we conclude that lidar has the potential to predict CBH in areas where there is a wide range of observed values. Naesset and Økland (2002) explained 71% of the variability in mean crown height in a boreal forest, where values had a range of 6.3 m. More work is

needed to generate useful models to predict this variable using lidar, as it is unclear why the best model selected in this study should describe CBH as proportional to the variability in stand height and inversely proportional to that height.

Some lidar studies have found nonlinear relationships between lidar metrics and aboveground biomass (Lefsky et al., 1999b, 2002a; Naesset, 2002) and basal area (Naesset, 2002). These were generally masked by the use of log-transformed equations, the use of squared or cubic values of the lidar metrics as predictor variables, and the presentation of plots of observed versus predicted, rather than field values versus lidar metric values. Our initial results seemed to support this: a nonlinear regression was the best model for all four biomass structure variables and canopy bulk density (Table 4). The predictor variable ($P_{G/1}$) is inversely related to canopy closure (Table 3). It is possible that in these forests with relatively low biomass density (Peet, 2000), the correlation between cover and biomass characteristics is stronger than in high biomass systems, where most lidar studies have been developed (Lefsky et al., 1999b; Means et al., 1999; Drake et al., 2002). This might explain the selection of this predictor variable.

However, there are factors that suggest that the selection of a nonlinear model to describe biomass structure could simply be an artifact of our sample. First, our field data were clumped at the lower end of the range of biomass structure and density values. Second, other studies have found increasing variability in the predictions of biomass from lidar metrics as biomass levels increase (Lefsky et al., 1999a,b; Drake et al., 2002). Third, the sites with greatest biomass values were the four sites with highest tree density. We estimated biomass from a sample of trees at these sites (see Section 2). At high density sites, this sample was a small proportion of the total tree population (three sites had less than 5% sample). Deviations between sample mean tree biomass and the true mean tree biomass were also inflated in these high density sites by the way we calculated per hectare biomass values. These factors, combined with outlier and leverage diagnostics, led us to refit and rerank the models without the four largest values plus one other leverage point, to test the sensitivity of the relationships to these sites (Table 6). The possibility that the error in four of these values is large led us to consider this a necessary step in arriving at our conclusions. This restriction of the domain tends to increase the fit of linear models. We have presented the most parsimonious models, based on the information provided by the information–theoretic approach (Table 6).

All the top models for total aboveground biomass are linear functions. Theoretically, the combination of a height metric with a cover metric provides the three-dimensional information needed to estimate biomass without saturation of the relationship at high biomass values. This supports the use of lidar to obtain nonsaturating relationships to estimate total biomass, though the values represented in this restricted dataset are within the range that can be estimated using optical sensors (<150 Mg/ha; Waring et al., 1995).

Our capacity to estimate basal area with lidar data is due to the correlation between basal area and total amount of reflecting surfaces in the stand (i.e. total biomass), rather than a direct measurement. Eight of the top models for basal area included an interaction term. The difficulty in clearly interpreting these models, combined with the similarity of some of the close competitors to the models selected for total aboveground biomass, led us to conclude that the most practical model to predict basal area in this system is a linear function of a height metric and a cover-related metric (Table 6). The selection of this model simplified the subset of potentially useful lidar metrics. The variability left unexplained by these models is likely also due to sampling error, given the methodology we used to estimate basal area.

The best model for tree density, selected with the restricted dataset, was still a nonlinear function of a metric inversely related to canopy cover (Table 6). These estimates were the least robust (Table 5). This could be due to errors in its estimation on the ground, particularly if trees are not randomly distributed, as assumed by the point-centered quarter method. It is possible to combine tree density and individual tree sizes in a variety of ways resulting in similar amounts of reflecting surfaces, which would also make it difficult to consistently predict density from lidar metrics. Naesset and Bjerknes (2001) found similar low fit for their regression model for density of young Norway spruce and Scots pine plantations. A close competitor to the best model (based on the restricted dataset) that had similar support and goodness of fit (r^2 and standard errors) was a linear function of the same lidar metric. We

therefore consider that there is potential for obtaining linear relationships to estimate tree density using discrete-return lidar. More work needs to be done in this area, since the indirectness of the relationship between the information gathered by the sensor and tree density might determine that relationships are consistent only over a very limited range of conditions.

Two of the top four models for foliage biomass were linear functions of the canopy cover metric in the original best model, combined with a height metric and the height to the base of the canopy metric. In both cases the confidence limits of the coefficient for the height metric straddled zero. A posteriori, we fit a linear regression based solely on the metrics related to cover and canopy base height ($r^2 = 58.7\%$; S.E. = 0.13). Its capacity to explain the variability in foliage biomass is a strong indicator of its potential for prediction, and should be considered in further studies of this kind. The linear function of the canopy cover metric in the original best model has a similar goodness of fit (Table 6), proving the most parsimonious a priori model. These results support the use of linear models to estimate foliage biomass from discrete-return lidar.

Canopy bulk density, critical for fire behavior modeling (Scott and Reinhardt, 2001), is related to foliage biomass and canopy volume. Our dataset is likely too small to provide parsimonious model selection (Burnham and Anderson, 2002). Though the best model was nonlinear, linear functions of the cover related metric ($P_{G/1}$) and a biomass density metric (δ_{12}) had slight support. We suggest that further studies aimed at estimating canopy bulk density will prove discrete-return lidar's capacity to estimate this variable with models that do not saturate at high values.

This exploratory analysis has allowed us to present regression models that explain a substantial portion of the variability in the stand structural variables we were interested in. We have also selected a subset of the 39 lidar metrics analyzed. Based on the best selected models, the position of confidence intervals of parameters relative to zero, the need to avoid overfitting the data and the capacity of metrics to predict a variety of structural variables, we have selected a subset of 14 lidar metrics (Table 7). We recommend that further studies concentrate on these metrics as useful predictors of stand structural variables in ponderosa pine forests.

Table 7
Lidar metrics that were useful predictors of stand structure variables

Stand structure variable represented	Useful predictors (lidar-based metrics[a])
Mean height	h_{max50}, h_{max95}, h_{max90}, h_{max25}, h_{max10}, SD_{h_3}, $range_{h_3}$
Lorey's height	h_{max25}, SD_{h_3}, $range_h$
Total aboveground biomass	h_{max95}, h_{max90}, CH, h_1, $P_{G/1}$, $P_{1/G}$
Foliage biomass	$P_{G/1}$, HC
Basal area	h_{max90}, h_{max95}, CH, h_1, $P_{G/1}$, $P_{1/G}$
Tree density	$P_{G/1}$, $P_{1/G}$
Canopy bulk density	$P_{G/1}$
Canopy base height	h_{1m}, h_{13}, SD_{h_3}, $range_{h_3}$

[a] Names of lidar metrics described in Table 3.

5. Conclusions

This study confirmed discrete-return lidar's capacity to measure stand height, and identified the fraction of the tallest 1st returns that directly relate to Lorey's height in these ponderosa pine forests. The selected linear models offer useful estimates of total aboveground biomass, basal area and foliage biomass. The models selected for tree density provide an initial estimate, though the lack of a direct relationship between characteristics measured by lidar sensors and this variable makes more research in this area necessary. Using lidar to predict canopy base height and canopy bulk density is still an unresolved issue. Our results suggest that there is potential, and studies with a greater number of samples, evenly stratified across the complete range of values found in these forests will hopefully identify the necessary predictor variables and functional relationships.

We identified a subset of lidar metrics that should be considered in future studies. The use of an information–theoretic approach to model selection provided us with a wealth of information on model and variable ranking. We consider this approach particularly useful, and its application to this study gives us confidence that the selected lidar metrics have potential as predictors of stand structure.

In a broader context, our results are consistent with other studies using lidar. We agree that lidar can provide estimates of forest biomass based on nonsaturating relationships, though we highlight the need to carefully interpret the results presented to support it. Our results also provide some insight into the importance of

carrying out lidar studies in a variety of ecosystems, and of broadening the focus of future studies to include low biomass forests, where the best lidar metrics may not be the same as in high density forests. Low biomass systems have been mostly neglected, as lidar studies have focused on accurately estimating high levels of biomass (Lefsky et al., 1999a; Drake et al., 2002), or on commercial forestry inventories (Naesset, 2002). We have addressed this issue, and our results support the need for more studies in low density systems.

The number of extreme fires in forests in the western United States highlights the need to increase our understanding of the effect of stand structure and its spatial arrangement on fire behavior. Spatially explicit estimates of tree density, canopy base height and canopy bulk density are required to focus efforts of forest restoration and fuels mitigation treatments. We hope that this will provide the necessary motivation for these studies to be carried out.

Acknowledgements

We would like to thank 3Di/EagleScan Inc. for providing the lidar data, and the Denver Water Board for access to the Cheesman Lake reservoir. Paula Fornwalt and Laurie Huckaby were extremely helpful with data collection methods. Two anonymous reviewers provided insightful criticisms. This research was supported by McIntyre Stennis and NASA funds, and a José A. Estenssoro Fellowship awarded to Sonia A. Hall by the YPF Foundation, Argentina.

Appendix A. Description and calculation of complex lidar metrics (see Table 3)

CRS: canopy reflection sum. *Rationale:* this metric is analogous to variable by the same name defined by Means et al. (1999).

$$\text{CRS} = \frac{\sum_{i=1}^{N} I_i}{A}$$

(for all symbol descriptions, see Table A.1).

rel-CRS$_1$: relative canopy reflection sum. *Rationale:* expressing CRS relative to the intensity of returns from the canopy and the ground should incorporate the effect of variations in canopy cover.

$$\text{rel-CRS}_1 = \frac{\sum_{i=1}^{N} I_i}{\sum_{i=1}^{T} I_i} \times \frac{1}{A}$$

rel-CRS$_2$: corrected relative canopy sum. *Rationale:* assuming the ground is covered in litter, the reflectance at 1064 nm of the ground is approximately half the reflectance of the green canopy (sensu Lefsky et al., 1999b).

$$\text{rel-CRS}_2 = \frac{\sum_{i=1}^{N} I_i}{\sum_{i=1}^{T} (I_i \times \rho)} \times \frac{1}{A}$$

Table A.1
Symbols used in equations for lidar metrics, described in Appendix A

Symbol	Definition
A	Area of the sampled site
M	Number of vegetation returns in a site with height >3 m
N	Total number of vegetation returns in a site
v	Number of vegetation returns within pulse i
T	Total number of returns (vegetation + ground) in a site
t	Total number of returns (vegetation or ground) within pulse i
I_i	Intensity (in raw counts) of return i
I_{ij}	Intensity of vegetation return j of pulse i
I_{ik}	Intensity of return k (vegetation or ground) of pulse i
z_i	Height above the ground of return i (ground returns have $z = 0$)
B_i	Sum of the standardized intensities of all returns classified as vegetation within height bin i. We standardized the intensities of all returns from one pulse, expressing the intensity of each return as the proportion of the total intensity returned for that particular pulse
h_i	Height above the ground of the midpoint of height bin i. We used 0.5 m height bins
max h	Total number of height bins, 0.5 m tall, in the site
CR_{1i}	Proportion of energy from pulse i returned by the canopy (i.e. in all vegetation returns)
CR_{2i}	Proportion of energy from pulse i returned by the canopy, corrected for variations in reflectance
P	Total number of pulses within a site
ρ	Reflectance factor: $\rho = 1$ for vegetation returns, $\rho = 2$ for ground returns

wCRS: the weighted canopy reflection sum. *Rationale:* number and size of trees taper off high in the canopy (i.e. less biomass). In the center of a crown one return may be representative of the area around it, this is less likely at higher points in the canopy. This metric weighs the intensity of each return by the inverse of the height of that return. This will weigh returns closer to the ground more heavily, potentially correcting for the attenuation of incoming radiation close to the ground. We limited the vegetation returns to those above 3 m, to avoid over-weighing returns from understory vegetation. It is necessary to divide the weighted sum by the area of the sample site to make this metric comparable across sites of variable area.

$$w\mathrm{CRS} = \left[\sum_{i=1}^{M}\left(I_i \times \frac{1}{z_i}\right)\right] \times \frac{1}{A}$$

QMCH: quadratic mean canopy height. *Rationale:* this metric is analogous to the variable by the same name defined by Lefsky et al. (1999b), modified to apply to discrete return lidar data. This metric is based on the standardized intensity of returns with heights >3 m. It is necessary to divide the weighted sum by the area of the sample site to make this metric comparable across sites of variable area.

$$\mathrm{QMCH} = \left[\sqrt{\sum_{i=1}^{\max h} B_i \times h_i^2}\right] \times \frac{1}{A}$$

CR_1: proportion of energy returned by the canopy. *Rationale:* analogous to the inverse of the ground return ratio defined by Drake et al. (2002), modified for discrete return lidar.

$$\text{for pulse } i,\ \mathrm{CR}_{1i} = \frac{\sum_{j=1}^{v} I_{ij}}{\sum_{k=1}^{t} I_{ik}};$$

$$\text{for the site},\ \mathrm{CR}_1 = \frac{\sum_{i=1}^{P} \mathrm{CR}_{1i}}{P}$$

CR_2: proportion of energy returned by the canopy, corrected for variations in reflectance (sensu Lefsky et al., 1999b).

$$\text{for pulse } i,\ \mathrm{CR}_{2i} = \frac{\sum_{j=1}^{v} I_{ij}}{\sum_{k=1}^{t} I_{ik} \times \rho};$$

$$\text{for the site},\ \mathrm{CR}_2 = \frac{\sum_{i=1}^{P} \mathrm{CR}_{2i}}{P}$$

Appendix B. Candidate regression models for each stand structural variable

Mean height and Lorey's height (h):

$$h = \beta_0 + \beta_1 h_x \quad (18)$$
$$h = \beta_0 + \beta_1 h_x + \beta_2 \mathrm{var}_x \quad (18 \times 4)$$
$$h = \beta_0 + \beta_1 h_x + \beta_2 \mathrm{var}_x + \beta_3 h_x \mathrm{var}_x \quad (18 \times 2)$$

(only absolute variability metrics)

For symbols used in equations see Table B.1.

Variability in tree heights could determine that measures of canopy surface height are not representative of the stand height. The compensating effect due to variability can be additive or multiplicative.

$$h = \beta_0 + \beta_1 h_{\mathrm{avg}} + \beta_2 h_{\mathrm{med}} \quad (9)$$
$$h = \beta_0 + \beta_1 h_{\mathrm{avg}} + \beta_2 h_{\mathrm{med}} + \beta_3 h_{\mathrm{med}} h_{\mathrm{avg}} \quad (9)$$

When tree height distributions are not normal, the difference between mean and median heights could

Table B.1
Symbols used in equations of candidate models for each stand structure variable, described in Appendix B

Symbol	Metric representative of
h_x	Tree or canopy heights
h_{avg}	Mean tree or canopy heights
h_{med}	Median canopy heights
var_x	Variability in canopy height
cover_x	Canopy cover
B_x	Biomass density
HC_x	Crown height
β_0, β_1, β_2, β_3, c	Regression coefficients

describe stand height better than only the mean. This effect can be additive or multiplicative.

$$h = \beta_1 h_x^c \quad (18)$$
$$h = \beta_0 + \beta_1 h_x^c \quad (18)$$

Canopy base height (CBH):

$$\mathrm{CBH} = \beta_0 + \beta_1 \mathrm{HC}_x \quad (1)$$
$$\mathrm{CBH} = \beta_0 + \beta_1 \mathrm{HC}_x^c \quad (1)$$
$$\mathrm{CBH} = \beta_1 \mathrm{HC}_x^c \quad (1)$$
$$\mathrm{CBH} = \beta_0 + \beta_1 \mathrm{HC}_x + \beta_2 \mathrm{var}_x \quad (4)$$
$$\mathrm{CBH} = \beta_0 + \beta_1 \mathrm{HC}_x + \beta_2 \mathrm{var}_x + \beta_1 \mathrm{HC}_x \mathrm{var}_x \quad (4)$$

Variability in tree heights may be related to variability in crown heights. Therefore, combining a measure of variability in height with the metric representing crown base height could better predict canopy base height. This effect can be additive or multiplicative.

$$\mathrm{CBH} = \beta_0 + \beta_1 h_x + \beta_2 \mathrm{HC}_x \quad (18)$$
$$\mathrm{CBH} = \beta_0 + \beta_1 h_x + \beta_2 \mathrm{HC}_x + \beta_3 h_x \mathrm{HC}_x \quad (18)$$

Since the lidar does not distinguish foliage from other biomass components, the representativeness of the lidar metric for crown base height might be dependent on stand height or age, described by a canopy height metric. This effect can be additive or multiplicative.

$$\mathrm{CBH} = \beta_0 + \beta_1 h_x \quad (18)$$
$$\mathrm{CBH} = \beta_0 + \beta_1 h_x^c \quad (0 \le c \le 1;\ c > 1) \quad (18 \times 2)$$
$$\mathrm{CBH} = \beta_1 h_x^c \quad (0 \le c \le 1;\ c > 1) \quad (18 \times 2)$$

As tree heights increase, so should height to crown, due to shading and dying of lower branches. The increase in these two measures might be proportional or not.

$$\mathrm{CBH} = \beta_0 + \beta_1 h_x + \beta_2 \mathrm{var}_x \quad (18 \times 4)$$
$$\mathrm{CBH} = \beta_0 + \beta_1 h_x + \beta_2 \mathrm{var}_x + \beta_3 h_x \mathrm{var}_x \quad (18 \times 2)$$

(only absolute variability metrics)

The proportionality in the relationship between tree heights and crown heights might vary at the stand level if the individual tree heights are more or less variable.

Total aboveground biomass (TAB):

$$\mathrm{TAB} = \beta_0 + \beta_1 B_x \quad (11)$$
$$\mathrm{TAB} = \beta_0 + \beta_1 B_x^c \quad (11)$$
$$\mathrm{TAB} = \beta_1 B_x^c \quad (11)$$
$$\mathrm{TAB} = \beta_0 + \beta_1 \mathrm{cover}_x \quad (5)$$
$$\mathrm{TAB} = \beta_0 + \beta_1 \mathrm{cover}_x^c \quad (5)$$
$$\mathrm{TAB} = \beta_1 \mathrm{cover}_x^c \quad (5)$$

Tree biomass in low density forests could be well represented by canopy cover, linearly or nonlinearly.

$$\mathrm{TAB} = \beta_0 + \beta_1 h_x^c \quad (0 \le c \le 1;\ c > 1) \quad (18 \times 2)$$
$$\mathrm{TAB} = \beta_1 h_x^c \quad (0 \le c \le 1;\ c > 1) \quad (18 \times 2)$$

Tree allometries indicate that tree biomass is related to tree height. As height is one-dimensional and biomass is three-dimensional, this relationship is likely to be nonlinear.

$$\mathrm{TAB} = \beta_0 + \beta_1 h_x + \beta_2 \mathrm{HC}_x \quad (18 \times 1)$$
$$\mathrm{TAB} = \beta_0 + \beta_1 h_x + \beta_2 \mathrm{HC}_x + \beta_3 h_x \mathrm{HC}_x \quad (18 \times 1)$$

The crown makes up an important part of the tree biomass. So the relationship between height and biomass might be more precise if we include information on how much of that height is part of the crown. This effect can be additive or multiplicative.

$$\mathrm{TAB} = \beta_0 + \beta_1 h_x + \beta_2 \mathrm{cover}_x + \beta_3 \mathrm{cover}_x h_x \quad (18 \times 5)$$
$$\mathrm{TAB} = \beta_0 + \beta_1 h_x + \beta_2 \mathrm{cover}_x \quad (18 \times 5)$$

Stand height and stand cover represent the three dimensions over which the biomass is distributed, so representing these two measures in a model could be used to describe stand biomass.

$$\mathrm{TAB} = \beta_0 + \beta_1 h_x + \beta_2 \mathrm{var}_x \quad (18 \times 4)$$
$$\mathrm{TAB} = \beta_0 + \beta_1 h_x + \beta_2 \mathrm{var}_x + \beta_3 h_x \mathrm{var}_x \quad (18 \times 2)$$

(only absolute variability metrics)

The greater the variability in heights in a stand, the more likely there are to be gaps in the canopy. These gaps may loosen the correlation between height and biomass, and this difference can be accounted for by a

measure of variability. This effect can be additive or multiplicative.

Foliage biomass (FB) and canopy bulk density (CBD): All the same regression models as for TAB, plus:

$$\text{FB/CBD} = \beta_0 + \beta_1 h_x + \beta_2 \text{cover}_x + \beta_3 \text{HC}_x \quad (18 \times 5)$$

The amount of foliage biomass should relate to crown height rather than tree height. Including a measure of height to crown will account for the difference.

Basal area (BA):

$$\text{BA} = \beta_0 + \beta_1 B_x \quad \text{(without } \delta_3\text{)} \quad (10)$$
$$\text{BA} = \beta_0 + \beta_1 B_x^c \quad \text{(without } \delta_3\text{)} \quad (10)$$
$$\text{BA} = \beta_1 B_x^c \quad \text{(without } \delta_3\text{)} \quad (10)$$
$$\text{BA} = \beta_0 + \beta_1 \text{cover}_x \quad (5)$$
$$\text{BA} = \beta_0 + \beta_1 \text{cover}_x^c \quad (5)$$
$$\text{BA} = \beta_1 \text{cover}_x^c \quad (5)$$
$$\text{BA} = \beta_0 + \beta_1 h_x \quad (18)$$
$$\text{BA} = \beta_0 + \beta_1 h_x^c \quad (18)$$
$$\text{BA} = \beta_1 h_x^c \quad (18)$$

Stand basal area relates to tree size (diameter and height) and tree density. These measures are also determinants of tree biomass and canopy cover. Therefore, biomass density, cover and height metrics should correlate with basal area.

$$\text{BA} = \beta_0 + \beta_1 h_x + \beta_2 B_x \quad \text{(without } \delta_3\text{)} \quad (18 \times 10)$$
$$\text{BA} = \beta_0 + \beta_1 h_x + \beta_2 B_x + \beta_3 h_x B_x \quad (18 \times 10)$$

If biomass is distributed over a large stand height, basal area may be smaller than expected based on stand biomass. Combining a height and a biomass density metric could therefore predict basal area more accurately than either on its own. This effect can be additive or multiplicative.

$$\text{BA} = \beta_0 + \beta_1 h_x + \beta_2 \text{cover}_x + \beta_3 h_x \text{cover}_x \quad (18 \times 5)$$
$$\text{BA} = \beta_0 + \beta_1 h_x + \beta_2 \text{cover}_x \quad (18 \times 5)$$

Canopy cover has an absolute maximum. Once this is reached, increases in height should correlate with increases in basal area that cannot be explained by canopy cover.

Tree density (δ):

$$\delta = \beta_0 + \beta_1 \text{cover}_x \quad (5+1)$$
$$(\beta_1 > 0 \text{ and } \beta_1 \leq 0 \text{ for } \delta_{11})$$
$$\delta = \beta_0 + \beta_1 \text{cover}_x^c \quad (5+1)$$
$$(\beta_1 > 0 \text{ and } \beta_1 \leq 0 \text{ for } \delta_{11})$$
$$\delta = \beta_1 \text{cover}_x^c \quad (5+1)$$
$$(\beta_1 > 0 \text{ and } \beta_1 \leq 0 \text{ for } \delta_{11})$$

The greater the number of trees, the greater the canopy cover. This relationship could be linear or nonlinear.

$$\delta = \beta_0 + \beta_1 \text{var}_x \quad (\beta_1 > 0 \text{ and } \beta_1 \leq 0) \quad (4 \times 2)$$
$$\delta = \beta_0 + \beta_1 \text{var}_x^c \quad (4)$$
$$\delta = \beta_1 \text{var}_x^c \quad (4)$$

Greater tree densities will favor competition. This could generate variability in individual tree growth, and therefore, variability in stand height.

$$\delta = \beta_0 + \beta_1 h_x^c \quad (18)$$
$$\delta = \beta_1 h_x^c \quad (18)$$

The older a stand, the greater the tree heights. Stand age should also correlate with variations in stand density. The correlation of both with stand age explains why stand height might be used to predict stand density.

References

Attiwill, P.M., 1994. The disturbance of forest ecosystems: the ecological basis for conservative management. Forest Ecol. Manage. 63, 247–300.

Baltsavias, E.P., 1999a. Airborne laser scanning: basic relations and formulas. ISPRS J. Photogramm. Rem. Sens. 54, 199–214.

Baltsavias, E.P., 1999b. Airborne laser scanning: existing systems and firms and other resources. ISPRS J. Photogramm. Rem. Sens. 54, 164–198.

Baret, F., Guyot, G., 1991. Potentials and limits of vegetation indexes for LAI and APAR assessment. Rem. Sens. Environ. 35, 161–173.

Brown, P.M., D'Amico, D.R., Carpenter, A.T., Andrews, D., 2001. Restoration of montane ponderosa pine forests in the Colorado Front Range. Ecol. Restoration 19, 19–26.

Burnham, K.P., Anderson, D.R., 2002. Model Selection and Multimodel Inference—A Practical Information–Theoretic Approach. Springer-Verlag, New York, USA.

Cohen, W.B., Spies, T.A., 1992. Estimating structural attributes of Douglas-fir/western hemlock forest stands from Landsat and SPOT imagery. Rem. Sens. Environ. 41, 1–17.

Cooper, C.F., 1960. Changes in vegetation, structure, and growth of southwestern pine forests since white settlement. Ecol. Monogr. 30, 129–164.

Cottam, G., Curtis, J.T., 1956. The use of distance measures in phytosociological sampling. Ecology 37, 451–460.

Covington, W.W., Moore, M.M., 1994. Postsettlement changes in natural fire regimes and forest structure: ecological restoration of old-growth ponderosa pine forests. In: Sampson, R.N., Adams, D.L. (Eds.), Assessing Forest Ecosystem Health in the Inland West. The Haworth Press Journal Co-Editions, New York, New York, USA, pp. 153–181.

DeGraaf, R.M., Hestbeck, J.B., Yamasaki, M., 1998. Associations between breeding bird abundance and stand structure in the White Mountains, New Hampshire and Maine, USA. Forest Ecol. Manage. 103, 217–233.

Dobson, M.C., 2000. Forest information from synthetic aperture radar. J. Forestry 98, 41–43.

Drake, J.B., Dubayah, R.O., Clark, D.B., Knox, R.G., Blair, J.B., Hofton, M.A., Chazdon, R.L., Weishampel, J.F., Prince, S.D., 2002. Estimation of tropical forest characteristics using large-footprint lidar. Rem. Sens. Environ. 79, 305–319.

Drake, J.B., Knox, R.G., Dubayah, R.O., Clark, D.B., Condit, R., Blair, J.B., Hofton, M., 2003. Above-ground biomass estimation in closed canopy Neotropical forests using lidar remote sensing: factors affecting the generality of relationships. Global Ecol. Biogeogr. 12, 147–159.

Dubayah, R.O., Drake, J.B., 2000. Lidar remote sensing for forestry. J. Forestry 98, 44–46.

Edminster, C.B., Beeson, R.T., Metcalf, G.E., 1980. Volume tables and point sampling factors for ponderosa pine in the Front Range of Colorado. USDA Forest Service Research Paper RM-218.

Flannigan, M.D., Van Wagner, C.E., 1991. Climate change and wildfire in Canada. Can. J. Forest Res. 21, 66–72.

Flood, M., Gutelius, B., 1997. Commercial implications of topographic terrain mapping using scanning airborne laser radar. Photogramm. Eng. Rem. Sens. 63, 327–366.

Franklin, S.E., 2001. Remote Sensing for Sustainable Forest Management. CRC Press LLC, Boca Raton, Florida, USA.

Fulé, P.Z., Waltz, A.E.M., Covington, W.W., Heinlein, T.A., 2001. Measuring forest restoration effectiveness in reducing hazardous fuels. J. Forestry 99, 24–29.

Gholz, H.L., Grier, C.C., Campbell, A.G., Brown, A.T., 1979. Equations for estimating biomass and leaf area of plants in the Pacific Northwest. Forest Research Lab, School of Forestry, Oregon State University. Research Paper 41.

Hershey, K.T., Meslow, E.C., Ramsey, F.L., 1998. Characteristics of forests at spotted owl nest sites in the Pacific Northwest. J. Wildl. Manage. 62, 1398–1410.

Holmgren, J., Nilsson, M., Olsson, H., 2003. Estimation of tree height and stem volume on plots using airborne laser scanning. Forest Sci. 49, 419–428.

Houghton, R.A., Hackler, J.L., Lawrence, K.T., 2000. Changes in terrestrial carbon storage in the United States. 2. The role of fire and fire management. Global Ecol. Biogeogr. 9, 145–170.

Hughes, R.F., Kauffman, J.B., Cummungs, D.L., 2000. Fire in the Brazilian Amazon. 3. Dynamics of biomass, C, and nutrient pools in regenerating forests. Oecologia 124, 574–588.

Husch, B., Beers, T.W., Kershaw Jr., J.A., 2003. Forest Mensuration. John Wiley and Sons Inc. Hoboken, New Jersey, USA.

Kaufmann, M.R., Regan, C.M., Brown, P.M., 2000. Heterogeneity in ponderosa pine/Douglas fir forests: age and size structure in unlogged and logged landscapes of central Colorado. Can. J. Forest Res. 30, 698–711.

Keane, R.E., Arno, S.F., Brown, J.K., 1990. Simulating cumulative fire effects in ponderosa pine/Douglas-fir forests. Ecology 71, 189–203.

Lefsky, M.A., Cohen, W.B., Acker, S.A., Parker, G.G., Spies, T.A., Harding, D., 1999a. Lidar remote sensing of the canopy structure and biophysical properties of Douglas-fir western hemlock forests. Rem. Sens. Environ. 70, 339–361.

Lefsky, M.A., Cohen, W.B., Harding, D.J., Parker, G.P., Acker, S.A., Gower, S.T., 2002a. Lidar remote sensing of above-ground biomass in three biomes. Global Ecol. Biogeogr. 11, 393–399.

Lefsky, M.A., Cohen, W.B., Parker, G.G., Harding, D.J., 2002b. Lidar remote sensing for ecosystem studies. BioScience 52, 19–30.

Lefsky, M.A., Cohen, W.B., Spies, T.A., 2001. An evaluation of alternate remote sensing products for forest inventory, monitoring, and mapping of Douglas fir forests in western Oregon. Can. J. Forest Res. 31, 78–87.

Lefsky, M.A., Harding, D., Cohen, W.B., Parker, G., Shugart, H.H., 1999b. Surface lidar remote sensing of basal area and biomass in deciduous forests of eastern Maryland, USA. Rem. Sens. Environ. 67, 83–98.

Lindgren, B.W., 1993. Statistical Theory. Chapman and Hall, New York, USA.

Magnussen, S., Boudewyn, P., 1998. Derivations of stand heights from airborne laser scanner data with canopy-based quantile estimators. Can. J. Forest Res. 28, 1016–1031.

Means, J.E., Acker, S.A., Fitt, B.J., Renslow, M., Emerson, L., Hendrix, C.J., 2000. Predicting forest stand characteristics with airborne scanning lidar. Photogramm. Eng. Rem. Sens. 66, 1367–1371.

Means, J.E., Acker, S.A., Harding, D.J., Blair, J.B., Lefsky, M.A., Cohen, W.B., Harmon, M.E., McKee, W.A., 1999. Use of large-footprint scanning airborne lidar to estimate forest stand characteristics in the Western Cascades of Oregon. Rem. Sens. Environ. 67, 298–308.

Moore, M.M., Covington, W.W., Fulé, P.Z., 1999. Reference conditions and ecological restoration: a southwestern ponderosa pine perspective. Ecol. Appl. 9, 1266–1277.

Naesset, E., 2002. Predicting forest stand characteristics with airborne scanning laser using a practical two-stage procedure and field data. Rem. Sens. Environ. 80, 88–99.

Naesset, E., Bjerknes, K.-O., 2001. Estimating tree heights and number of stems in young forest stands using airborne laser scanner data. Rem. Sens. Environ. 78, 328–340.

Naesset, E., Økland, T., 2002. Estimating tree height and tree crown properties using airborne scanning laser in a boreal nature reserve. Rem. Sens. Environ. 79, 105–115.

Overpeck, J.T., Rind, D., Goldberg, R., 1990. Climate-induced changes in forest disturbance and vegetation. Nature 343, 51–53.

Page, S.E., Slegert, F., Rieley, J.O., Boehm, H.-D.V., Jaya, A., Limin, S., 2002. The amount of carbon released from peat and forest fires in Indonesia during 1997. Nature 420, 61–65.

Paré, D., Bergeron, Y., 1995. Above-ground biomass accumulation along a 230-year chronosequence in the southern portion of the Canadian boreal forest. J. Ecol. 83, 1001–1007.

Peet, R.K., 2000. Forests and meadows of the Rocky Mountains. In: Barbour, M.G., Billings, W.D. (Eds.), North American Terrestrial Vegetation. Cambridge University Press, Cambridge, UK.

Perry, G.L.W., 1998. Current approaches to modelling the spread of wildland fire: a review. Prog. Phys. Geogr. 22, 222–245.

Sando, R.W., Wick, C.H., 1972. A method of evaluating crown fuels in forest stands. U.S. Forest Service Research Paper, p. 10.

Scott, J.H., Reinhardt, E.D., 2001. Assessing crown fire potential by linking models of surface and crown fire behavior. USDA Forest Service Research Paper RMRS-RP-29.

Spanner, M., Johnson, L., Miller, J., McCreight, R., Fremantle, J., Runyon, J., Gong, P., 1994. Remote sensing of seasonal leaf area index across the Oregon transect. Ecol. Appl. 4, 258–271.

Sprugel, D.G., 1983. Correcting for bias in log-transformed allometric equations. Ecology 64, 209–210.

Stoker, J.M., 2002. Evaluating small-footprint multiple-return lidar to indentify individual tree characteristics. Thesis. Colorado State University, Fort Collins, Colorado, USA.

Ter-Mikaelian, M.T., Korzukhin, M.D., 1997. Biomass equations for sixty-five North American tree species. Forest Ecol. Manage. 97, 1–24.

Tilman, D., Reich, P., Phillips, H., Menton, M., Patel, A., Vos, E., Peterson, D., Knops, J., 2000. Fire suppression and ecosystem carbon storage. Ecology 81, 2680–2685.

van Wagner, C.E., 1977. Conditions for the start and spread of crown fire. Can. J. Forest Res. 7, 23–34.

van Wagner, C.E., 1993. Prediction of crown fire in two stands of jack pine. Can. J. Forest Res. 23, 442–449.

Waring, R.H., Way, J.B., Hunt Jr., E.R., Morrissey, L., Ranson, K.J., Weishampel, J.F., Oren, R., Franklin, S.E., 1995. Imaging radar for ecosystem studies. BioScience 45, 715–723.

Weaver, H., 1959. Ecological changes in the ponderosa pine forest of the Warm Springs Indian Reservation on Oregon. J. Forestry 57, 15–20.

Wirth, C., Schulze, E.-D., Schulze, W., von Stunzner-Karbe, D., Ziegler, W., Miljukova, I.M., Sogatchev, A., Varlagin, A.B., Panvyorov, M., Grigoriev, S., Kusnetzova, W., Siry, M., Hardes, G., Zimmermann, R., Vygodskaya, N.N., 1999. Above-ground biomass and structure of pristine Siberian Scots pine forests as controlled by competition and fire. Oecologia 121, 66–80.

Wulder, M., 1998. Optical remote-sensing techniques for the assessment of forest inventory and biophysical parameters. Prog. Phys. Geogr. 22, 449–476.